Evaluation of quantum image processing in CUDA-based simulation

Akira Hasegawa[a], Yoshihiro Maeda[b], and Norishige Fukushima[a]

[a]Nagoya Institute of Technology, Japan
[b]Shibaura Institute of Technology, Japan

ABSTRACT

Quantum computers are expected to be the next-generation computers in various fields. Quantum computers are different from classical computers, which store the current binary information of 0 and 1. Quantum computers can use quantum superposition, which can hold 0 to 1 probability as continuous quantities in one qubit. Therefore, existing algorithms are not necessarily efficient computational algorithms on quantum computers. GPU-based quantum simulations, such as cuQuantum, have recently been released to develop quantum algorithms. This paper focuses on quantum image processing, presents how far quantum image processing can be efficiently described today and verifies on GPUs that multiple image processing can be described using cuQuantum.

Keywords: Quantum Image Processing, Quantum Computer, cuQuantum

1. INTRODUCTION

The quantum computer that uses the quantum superposition property[1] is expected to be the next generation computer in various fields.[2,3] While classical computers could only take digital bits (0 or 1), quantum computers can use qubits (i.e., quantum superposition state), which have a coherent superposition of multiple states simultaneously until it is measured.

Then, it can probabilistically take either 0 or 1 by observation. By using these qubits to perform a large number of calculations in parallel, the computing speed of a quantum computer can be significantly faster than that of a classical computer. While classical computers use SIMD and multi-core threading,[4] tiling[5] and pipeline burst cache pipelining,[6] GPUs and Tensor Cores[7] for parallel computing.

Due to superposition for parallel computing, existing algorithms are not necessarily efficient computational algorithms on a quantum computer, requiring a new discussion of quantum algorithms. Due to the lack of easy access to quantum computers, the superiority of quantum computers over classical computers (quantum supremacy) could only be demonstrated in a limited number of applications, such as combinatorial optimization problems and prime factorization. However, around 2020, quantum simulators[8] are accelerated by GPUs, such as NVIDIA's cuQuantum and Microsoft's Azure Quantum, and then we can develop quantum algorithms without the need for quantum computers.

In this paper, we focus on image processing using a quantum computer (i.e., quantum image processing).[9–11] Quantum image processing is also at the beginning stage of research on quantum image representation and quantum image processing algorithms, which include how to realize simple processes such as edge detection[12] and how to store grayscale and color images in qubits.[13] Quantum image representation[14] has various forms: qubit lattice,[15] entangled image,[16] real ket,[17] flexible representation of quantum images (FRQI),[18] novel enhanced quantum representation of digital images (NEQR).[19] We use three representations, qubit lattice, FRQI, and NEQR, to show examples of image processing.

Corresponding author, N. Fukushima (E-mail: fukushima@nitech.ac.jp)

2. PRELIMINARY

2.1 Quantum states

A single qubit is a basic unit of quantum information handled by a quantum computer, and the quantum state $|\psi_1\rangle$ of one qubit is represented by a linear combination of $|0\rangle$ and $|1\rangle$ with two complex numbers α and β as in (1). The qubit $|\psi_1\rangle$ represents the superposition between 0 and 1 by these complex numbers α and β, called probability amplitudes or complex probability amplitudes. The probability of sampling 0 is $|\alpha|^2$, and for 1, $|\beta|^2$.

$$|\psi_1\rangle = \alpha \begin{pmatrix} 1 \\ 0 \end{pmatrix} + \beta \begin{pmatrix} 0 \\ 1 \end{pmatrix} = \alpha |0\rangle + \beta |1\rangle \quad (\alpha, \beta \in \mathbb{C}, |\alpha|^2 + |\beta|^2 = 1) \tag{1}$$

2.2 Quantum gates

While logical gates in a classical computer refer to a logic circuit that performs basic logic operations such as AND and OR operations, quantum gates replace conventional gates with ones with quantum characteristics.

Because of the constraint that the probability amplitude of a qubit satisfies the normalization condition even after applying a quantum gate, the quantum gate is mathematically represented by a unitary matrix.

The gates used in this paper are the Hadamard gate (H), phase shift gate (R_m), controlled X gate (CX), and Fredkin gate (F), shown below as matrices and the quantum gate symbols are shown in Fig 1. Here, $|c\rangle$ represents the control bit, which switches whether the quantum gate is applied. $|t\rangle$ denotes the target bit, which is the qubit to which the quantum gate is applied. When the control bit is $|0\rangle$, nothing is done to the target bit, and when $|1\rangle$, the specified quantum gate is applied to the target bit.

$$H = \frac{1}{\sqrt{2}} \begin{bmatrix} 1 & 1 \\ 1 & -1 \end{bmatrix}, \qquad R_m = \begin{bmatrix} 1 & 0 & 0 & 0 \\ 0 & 1 & 0 & 0 \\ 0 & 0 & 1 & 0 \\ 0 & 0 & 0 & e^{i\frac{2\pi}{2^m}} \end{bmatrix},$$
$$CX = \begin{bmatrix} 1 & 0 & 0 & 0 \\ 0 & 1 & 0 & 0 \\ 0 & 0 & 0 & 1 \\ 0 & 0 & 1 & 0 \end{bmatrix}, \qquad F = \begin{bmatrix} 1 & 0 & 0 & 0 & 0 & 0 & 0 & 0 \\ 0 & 1 & 0 & 0 & 0 & 0 & 0 & 0 \\ 0 & 0 & 1 & 0 & 0 & 0 & 0 & 0 \\ 0 & 0 & 0 & 1 & 0 & 0 & 0 & 0 \\ 0 & 0 & 0 & 0 & 1 & 0 & 0 & 0 \\ 0 & 0 & 0 & 0 & 0 & 0 & 1 & 0 \\ 0 & 0 & 0 & 0 & 0 & 1 & 0 & 0 \\ 0 & 0 & 0 & 0 & 0 & 0 & 0 & 1 \end{bmatrix}. \tag{2}$$

The Hadamard gate H produces a quantum superposition such that $H|0\rangle = \frac{1}{\sqrt{2}}(|0\rangle + |1\rangle)$. The phase shift gate R_m is a 2-input 2-output quantum gate with one control bit and one target bit as inputs, which changes the phase of the target bit by $\frac{2\pi}{2^m}$ when $|c\rangle = |1\rangle$. The controlled X gate CX is a 2-input 2-output quantum gate with one control bit and one target bit as inputs, which inverts the target bit from the state $|t\rangle = |0\rangle$ to $|t\rangle = |1\rangle$ when $|c\rangle = |1\rangle$. The Fredkin gate F is a three-input, three-output quantum gate with one control bit and two target bits as inputs, which swaps the quantum states of the two target bits from the states of $|t_1\rangle = |0\rangle$ and $|t_2\rangle = |1\rangle$ to $|t_1\rangle = |1\rangle$ and $|t_2\rangle = |0\rangle$ when $|c\rangle = |1\rangle$.

2.3 Qubit lattice

Qubit latice[15] is an early quantum image representation proposed by Venegas-Andraca in 2003, which does not use spatial quantum superposition or other quantum properties. Instead, the image is represented by mapping the probability amplitude of a single qubit to each pixel value. Therefore, the qubit lattice format requires the same number of qubits as pixels. The pixel value of the ith row and jth column in the classical image representation is represented in qubit lattice as follows.

$$|pixel_{i,j}\rangle = \cos\left(\frac{\theta_{i,j}}{2}\right)|0\rangle + \sin\left(\frac{\theta_{i,j}}{2}\right)|1\rangle, \quad 0 \le \theta_{i,j} \le \pi \tag{3}$$

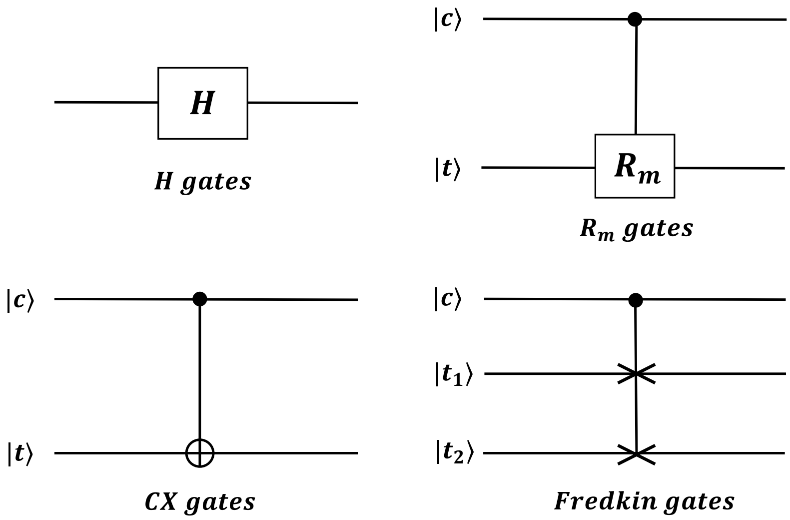

Figure 1: Quantum gate notations.

2.4 FRQI

Le et al. extended the qubit lattice to FRQI,[18] representing the pixel value and position by the quantum superposition. Similar to qubit lattice, pixel values are represented by a single qubit $\cos\frac{\theta_i}{2}|0\rangle + \sin\frac{\theta_i}{2}|1\rangle$ and the corresponding pixel position is represented by a qubit $|i\rangle$. The two pieces of information are represented using qubits, and the image is represented by taking the tensor product $\otimes$. The image representation using FRQI is formulated as follows

$$|I\rangle = \frac{1}{2^n}\sum_{i=0}^{2^{2n}-1}\left(\cos\frac{\theta_i}{2}|0\rangle + \sin\frac{\theta_i}{2}|1\rangle\right)\otimes|i\rangle, \quad 0 \le \theta_i \le \pi \tag{4}$$

The FRQI representation is a direct development of flexible representation for quantum color image (FRQCI)[20] and improved FRQI (IFRQI).[21] In addition, Sovel edge detection[22] and global and local image shifting[23] are presented.

2.5 NEQR

Zhang et al. proposed a quantum image representation called NEQR[19] that further extends FRQI. Like FRQI, this representation format focuses on pixel values and their corresponding positions. Unlike FRQI, it uses multiple qubits to represent pixel values. When the maximum pixel value is represented by 2^d, that is, when the pixel value can be represented as $C_x^0 C_x^1 \dots C_x^{d-1}$ in binary representation, the image can be represented using NEQR as follows.

$$|I\rangle = \frac{1}{2^n}\sum_{x=0}^{2^{2n}-1}|f(x)\rangle|x\rangle, \quad f(x) = C_x^0 C_x^1 ... C_x^{d-1}. \tag{5}$$

NEQR has evolved into improved NEQR (INEQR),[24] generilized model of NEQR (GNEQR),[25] etc. In addtion, edge detection,[26] feature extruction,[27] and color representation[28] are presented.

2.6 Quantum Fourier transform

The Fourier transform is an important image processing operation, and the quantum Fourier transform (QFT)[29] corresponds to the quantum properties of the Fourier transform. The fast Fourier transform (FFT) of a classical computer has $\mathcal{O}(N\log N)$ order, whereas the QFT can be calculated in $\mathcal{O}(\log^2 N)$. QFT is used in various quantum algorithms, and it can be realized by constructing a quantum circuit as shown in Fig. 2 using two

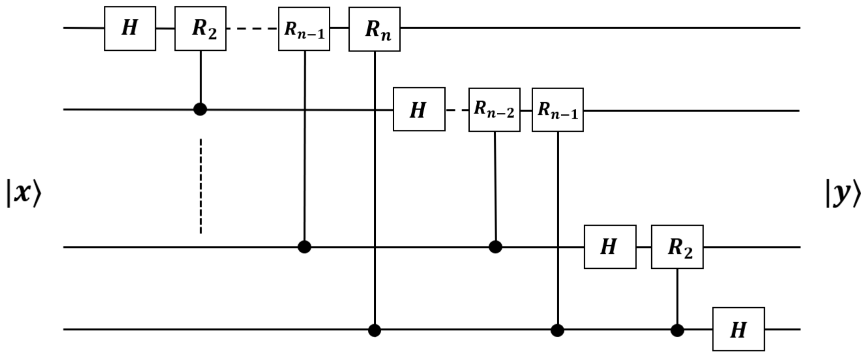

Figure 2: Quantum circuit for QFT.

quantum gates: a Hadamard gate H and a phase shift gate R_m. However, since this circuit outputs an inverted bit order, a swap gate must be added at the end of the quantum circuit to correct the bit order. Various frequency transforms have also been realized, such as the quantum Haar wavelet transform and the quantum Hadamard transform.[30]

3. QUANTUM IMAGE PROCESSING WITH VARIOUS QUANTUM IMAGE REPRESENTATIONS

3.1 Thresholding with qubit lattice

Because qubit lattice represents images without using spatial superposition, it can only perform simple operations such as rotation manipulation on a single qubit. In this section, we consider the binarization process to be realized by performing rotation operations per a qubit. The output value is determined by comparing the pixel value c and the threshold value r, as in the binarization process on a classical computer. When sampling is performed, the probability amplitude of the qubit must be manipulated to obtain a high probability value according to the result of the thresholding process since the qubit outputs 0 and 1 values probabilistically due to its characteristics. Therefore, we define a quantum gate R for rotation manipulation as follows for each case of $c < r$ and $r \leq c$, and apply this quantum gate to bias the probability amplitude to obtain a value with high probability according to the threshold processing result at sampling.

$$R = \begin{cases} \begin{bmatrix} \cos\frac{\pi}{4} & -\sin\frac{\pi}{4} \\ \sin\frac{\pi}{4} & \cos\frac{\pi}{4} \end{bmatrix} & (r \leq c) \\ \\ \begin{bmatrix} \cos\left(-\frac{\pi}{4}\right) & -\sin\left(-\frac{\pi}{4}\right) \\ \sin\left(-\frac{\pi}{4}\right) & \cos\left(-\frac{\pi}{4}\right) \end{bmatrix} & (c < r) \end{cases} \tag{6}$$

3.2 QFT with FRQI

FRQI maps pixel values to a single qubit probability amplitude. If each pixel value is placed as C_k and the pixel position is represented by $|k\rangle$, the image is represented as follows.

$$|I\rangle = \sum_{k=0}^{2^n-1} C_k |k\rangle = \begin{bmatrix} C_0 & C_1 & C_2 & \cdots & C_k \end{bmatrix}^{\mathsf{T}} \tag{7}$$

FRQI can represent the entire image as a superposition of qubits $|I\rangle$, which is suitable for the same processing on the entire image. In this paper, we implement QFT in FRQI to process the whole image. The following matrix

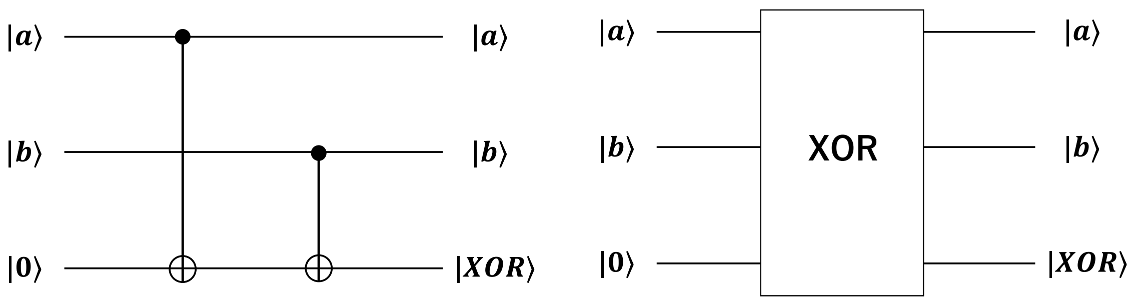

(a) XOR gate (b) abstructed XOR gate

Figure 3: XOR quantum circuit.

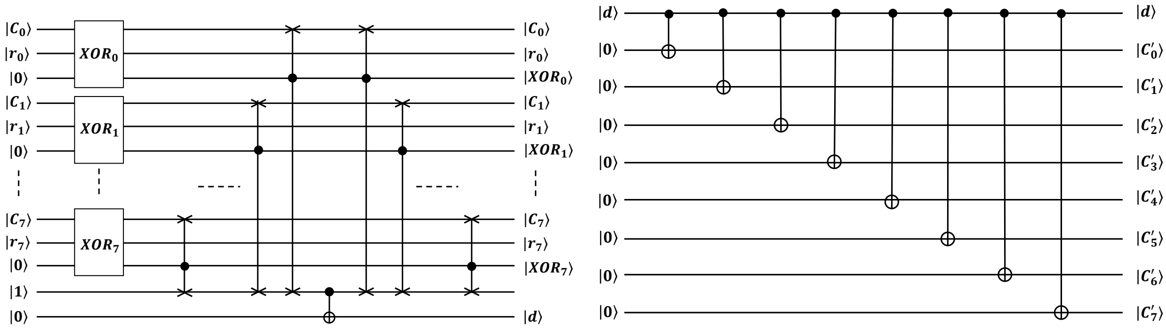

(a) Large and small comparisons (b) Pixel value determination

Figure 4: Quantum circuit for thresholding with NEQR.

can represent the size-N QFT.

$$QFT_N = \frac{1}{\sqrt{N}} \begin{bmatrix} 1 & 1 & 1 & 1 & \cdots & 1 \\ 1 & W_N & W_N^2 & W_N^3 & \cdots & W_N^{N-1} \\ 1 & W_N^2 & W_N^4 & W_N^6 & \cdots & W_N^{2(N-1)} \\ 1 & W_N^3 & W_N^6 & W_N^9 & \cdots & W_N^{3(N-1)} \\ \vdots & \vdots & \vdots & \vdots & \ddots & \vdots \\ 1 & W_N^{N-1} & W_N^{2(N-1)} & W_N^{3(N-1)} & \cdots & W_N^{(N-1)(N-1)} \end{bmatrix}, \quad W_N = e^{i\frac{2\pi}{N}} \tag{8}$$

3.3 Threshoding with NEQR

NEQR uses multiple qubits to represent pixel values. Therefore, more complex qubit manipulations are possible than with qubit lattice and FRQI, which increases the implementation variety of image processing algorithms. The thresholding is also performed with NEQR to confirm the possibility of the complex operations.

We consider the representation of a grayscale pixel value in NEQR with 8 qubits. First, we show that the XOR gate used for processing can be constructed using two controlled X gates and one auxiliary qubit. As shown in Fig. 3(a), $|a\rangle$ and $|b\rangle$ can be used as control bits, and the auxiliary qubits can be used as target bits to obtain the XOR result of $|a\rangle$ and $|b\rangle$ by acting two control X gates. The XOR circuit is abbreviated as shown in Fig. 3(b) in the following. Next, the binarization procedure is described. The quantum circuit shown in Fig.4(a) determines whether the pixel value is greater than or less than the threshold value. Here, the pixel value is denoted by $C = C_0C_1...C_7$ and the threshold value by $r = r_0r_1...r_7$ in binary. The quantum circuit in Fig. 4(a) uses XOR to determine which qubits are different for each digit. If $C \geq r$ is set to 1 and $C < r$ is set to 0, the highest C_i value for which the XOR value is 1 equals the value for which the large or small judgment result.

Therefore, using the Fredkin gate, the auxiliary qubits whose initial state represents $|1\rangle$ and the quantum state of C_i are swapped, starting from the lower bits. The value of $|d\rangle$, which represents the result of a large or small judgment, is determined using the control X gate based on the value of the auxiliary qubit after the swap. Then, based on $|d\rangle$, the output qubit $|C'\rangle$ is changed to 0 or 255 using the quantum circuit shown in Fig. 4(b). This quantum circuit requires a total of 18 auxiliary qubits: 8 qubits to realize XOR, 2 qubits for large and small comparisons, and 8 qubits to store the pixel values resulting from the thresholding process.

4. EXPERIMENTAL RESULTS

GPU-based simulations were performed using NVIDIA GeForce RTX 3060 with cuQuantum SDK. The image processing results for each image representation are shown.

Qubit lattice: Figure 5 shows the result of thresholding with qubit lattice. Although the application of quantum gates increases the probability of outputting a value that corresponds to the thresholding result for the entire image, there are cases where an incorrect value is output because the error probability is not zero. This error has an effect, resulting in a noisy grayscale image when the number of sampling times is negligible.

FRQI: Figure 6 shows the result of performing QFT with FRQI, phase-shifting the frequency image by $\frac{\pi}{8}$ using the phase shift gate, and then performing invert QFT. The result is an output with reduced pixel values and contrast.

NEQR: Figure 7 shows the result of thresholding with NEQR. When correcting the errors of the qubits in the quantum circuit is possible, NEQR can achieve more accurate binarization than a qubit lattice. It can perform more complex calculations since NEQR uses multiple qubits to represent pixel values. If the complexity of the quantum circuits is not considered, it can perform image processing algorithms similar to those of classical computers. However, depending on the quantum circuits used, the circuits may be more profound and require many auxiliary qubits.

5. CONCLUSION

In this paper, image processing was performed on three quantum image representations: qubit lattice, FRQI, and NEQR. Considering the characteristics of each quantum image representation, we performed thresholding for qubit lattice and NEQR and QFT for FRQI. In addition to the quantum image representation used in this paper, various other representation formats exist. Each has its characteristics, such as how to represent pixel values and pixel positions and how many qubits are used in the representation. The challenge for the future is to realize the representation with fewer quantum gates according to the characteristics of each representation.

ACKNOWLEDGMENTS

This research was supported by JSPS KAKENHI Grant Number JP21H03465, JP24K02960 and Environment Research and Technology Development Fund (JPMEERF20222M01) of the Environmental Restoration and Conservation Agency of Japan.

REFERENCES

[1] Monroe, C., Meekhof, D. M., King, B. E., and Wineland, D. J., "A "schrödinger cat" superposition state of an atom," *Science* **272**(5265), 1131–1136 (1996). https://doi.org/10.1126/science.272.5265.1131.

[2] Benioff, P., "The computer as a physical system: A microscopic quantum mechanical hamiltonian model of computers as represented by turing machines," *Journal of Statistical Physics* **22**, 563–591 (1980). https://doi.org/10.1007/BF01011339.

[3] Nielsen, M. A. and Chuang, I. L., [*Quantum computation and quantum information*], Cambridge university press (2010).

[4] Maeda, Y., Fukushima, N., and Matsuo, H., "Taxonomy of vectorization patterns of programming for fir image filters using kernel subsampling and new one," *Applied Sciences* **8**(8) (2018). https://doi.org/10.3390/app8081235.

(a) input (b) output

Figure 5: Resulting image of thresholding with qubit lattice.

(a) input (b) output

Figure 6: Resulting image of QFT with FRQI.

(a) input (b) output

Figure 7: Resulting image of thresholding with NEQR.

[5] Sugimoto, K., Fukushima, N., and Kamata, S., "200 fps constant-time bilateral filter using svd and tiling strategy," in *Proceedings of IEEE International Conference on Image Processing (ICIP)*, (2019). https://doi.org/10.1109/ICIP.2019.8802927.

[6] Fukushima, N., Maeda, Y., Kawasaki, Y., Nakamura, M., Tsumura, T., Sugimoto, K., and Kamata, S., "Efficient computational scheduling of box and gaussian fir filtering for cpu microarchitecture," in *Proceedings of Asia-Pacific Signal and Information Processing Association Annual Summit and Conference (APSIPA ASC)*, (2018). https://doi.org/10.23919/APSIPA.2018.8659674.

[7] Kondo, T., Maeda, Y., and Fukushima, N., "Accelerating finite impulse response filtering using tensor cores," in *Proceedings of Asia-Pacific Signal and Information Processing Association Annual Summit and Conference (APSIPA ASC)*, (2021).

[8] Georgescu, I. M., Ashhab, S., and Nori, F., "Quantum simulation," *Reviews of Modern Physics* **86**(1), 153 (2014). https://doi.org/10.1103/RevModPhys.86.153.

[9] Vlasov, A. Y., "Quantum computations and images recognition," *arXiv preprint quant-ph/9703010* (1997). https://doi.org/10.48550/arXiv.quant-ph/9703010.

[10] Wang, Z., Xu, M., and Zhang, Y., "Review of quantum image processing," *Archives of Computational Methods in Engineering* **29**(2), 737–761 (2022). https://doi.org/10.1007/s11831-021-09599-2.

[11] Anand, A., Lyu, M., Baweja, P. S., and Patil, V., "Quantum image processing," *arXiv preprint arXiv:2203.01831* (2022). https://doi.org/10.48550/arXiv.2203.01831.

[12] Ma, Y., Ma, H., and Chu, P., "Demonstration of quantum image edge extration enhancement through improved sobel operator," *IEEE Access* **8**, 210277–210285 (2020). https://doi.org/10.1109/ACCESS.2020.3038891.

[13] Giovannetti, V., Lloyd, S., and Maccone, L., "Quantum random access memory," *Physical Review Letters* **100**(16), 160501 (2008). https://doi.org/10.1103/PhysRevLett.100.160501.

[14] Lisnichenko, M. and Protasov, S., "Quantum image representation: A review," *Quantum Machine Intelligence* **5**(1), 2 (2023). https://doi.org/10.1007/s42484-022-00089-7.

[15] Venegas-Andraca, S. E. and Bose, S., "Storing, processing, and retrieving an image using quantum mechanics," in *Proceedings of SPIE, Quantum Information and Computation*, **5105**, 137–147 (2003). https://doi.org/10.1117/12.485960.

[16] Venegas-Andraca, S. E., Bose, S., et al., "Quantum computation and image processing: New trends in artificial intelligence," in *Proceedings of International Joint Conference on Artificial Intelligence (IJCAI)*, (2003). https://doi.org/10.5555/1630659.1630935.

[17] Latorre, J. I., "Image compression and entanglement," *arXiv preprint quant-ph/0510031* (2005). https://doi.org/10.48550/arXiv.quant-ph/0510031.

[18] Le, P. Q., Dong, F., and Hirota, K., "A flexible representation of quantum images for polynomial preparation, image compression, and processing operations," *Quantum Information Processing* **10**, 63–84 (2011). https://doi.org/10.1007/s11128-010-0177-y.

[19] Zhang, Y., Lu, K., Gao, Y., and Wang, M., "Neqr: a novel enhanced quantum representation of digital images," *Quantum Information Processing* **12**, 2833–2860 (2013). https://doi.org/10.1007/s11128-013-0567-z.

[20] Li, P., Xiao, H., and Li, B., "Quantum representation and watermark strategy for color images based on the controlled rotation of qubits," *Quantum Information Processing* **15**(11), 4415–4440 (2016). https://doi.org/10.1007/s11128-016-1413-x.

[21] Khan, R. A., "An improved flexible representation of quantum images," *Quantum Information Processing* **18**, 1–19 (2019). https://doi.org/10.1007/s11128-019-2306-6.

[22] Zhang, Y., Lu, K., and Gao, Y., "Qsobel: A novel quantum image edge extraction algorithm," *Science China Information Sciences* **58**, 1–13 (2015). https://doi.org/10.1007/s11432-014-5158-9.

[23] Zhou, R.-G., Tan, C., and Ian, H., "Global and local translation designs of quantum image based on frqi," *International Journal of Theoretical Physics* **56**, 1382–1398 (2017). https://doi.org/10.1007/s10773-017-3279-9.

[24] Zhou, R., Hu, W., Luo, G., Liu, X., and Fan, P., "Quantum realization of the nearest neighbor value interpolation method for ineqr," *Quantum Information Processing* **17**, 1–37 (2018). https://doi.org/10.1007/s11128-018-1921-y.

[25] Li, H.-S., Chen, X., Song, S., Liao, Z., and Fang, J., "A block-based quantum image scrambling for gneqr," *IEEE Access* **7**, 138233–138243 (2019). https://doi.org/10.1109/ACCESS.2019.2942986.

[26] Chetia, R., Boruah, S., and Sahu, P., "Quantum image edge detection using improved sobel mask based on neqr," *Quantum Information Processing* **20**(1), 21 (2021). https://doi.org/10.1007/s11128-020-02944-7.

[27] Zhang, Y., Lu, K., Xu, K., Gao, Y., and Wilson, R., "Local feature point extraction for quantum images," *Quantum Information Processing* **14**, 1573–1588 (2015). https://doi.org/10.1007/s11128-014-0842-7.

[28] Sang, J., Wang, S., and Li, Q., "A novel quantum representation of color digital images," *Quantum Information Processing* **16**, 1–14 (2017). https://doi.org/10.1007/s11128-016-1463-0.

[29] Coppersmith, D., "An approximate fourier transform useful in quantum factoring," *IBM Research Report* **RC 19642** (1994). https://doi.org/10.48550/arXiv.quant-ph/0201067.

[30] Yao, X.-W., Wang, H., Liao, Z., Chen, M.-C., Pan, J., Li, J., Zhang, K., Lin, X., Wang, Z., Luo, Z., et al., "Quantum image processing and its application to edge detection: Theory and experiment," *Physical Review X* **7**(3), 031041 (2017). https://doi.org/10.1103/PhysRevX.7.031041.